

ISCI, Volume 20

## **Supplemental Information**

**Aggregate Interactome Based on Protein**

**Cross-linking Interfaces Predicts Drug Targets to**

**Limit Aggregation in Neurodegenerative Diseases**

**Meenakshisundaram Balasubramaniam, Srinivas Ayyadevara, Akshatha Ganne, Samuel Kakraba, Narsimha Reddy Penthalala, Xiuxia Du, Peter A. Crooks, Sue T. Griffin, and Robert J. Shmookler Reis**

Figure S1

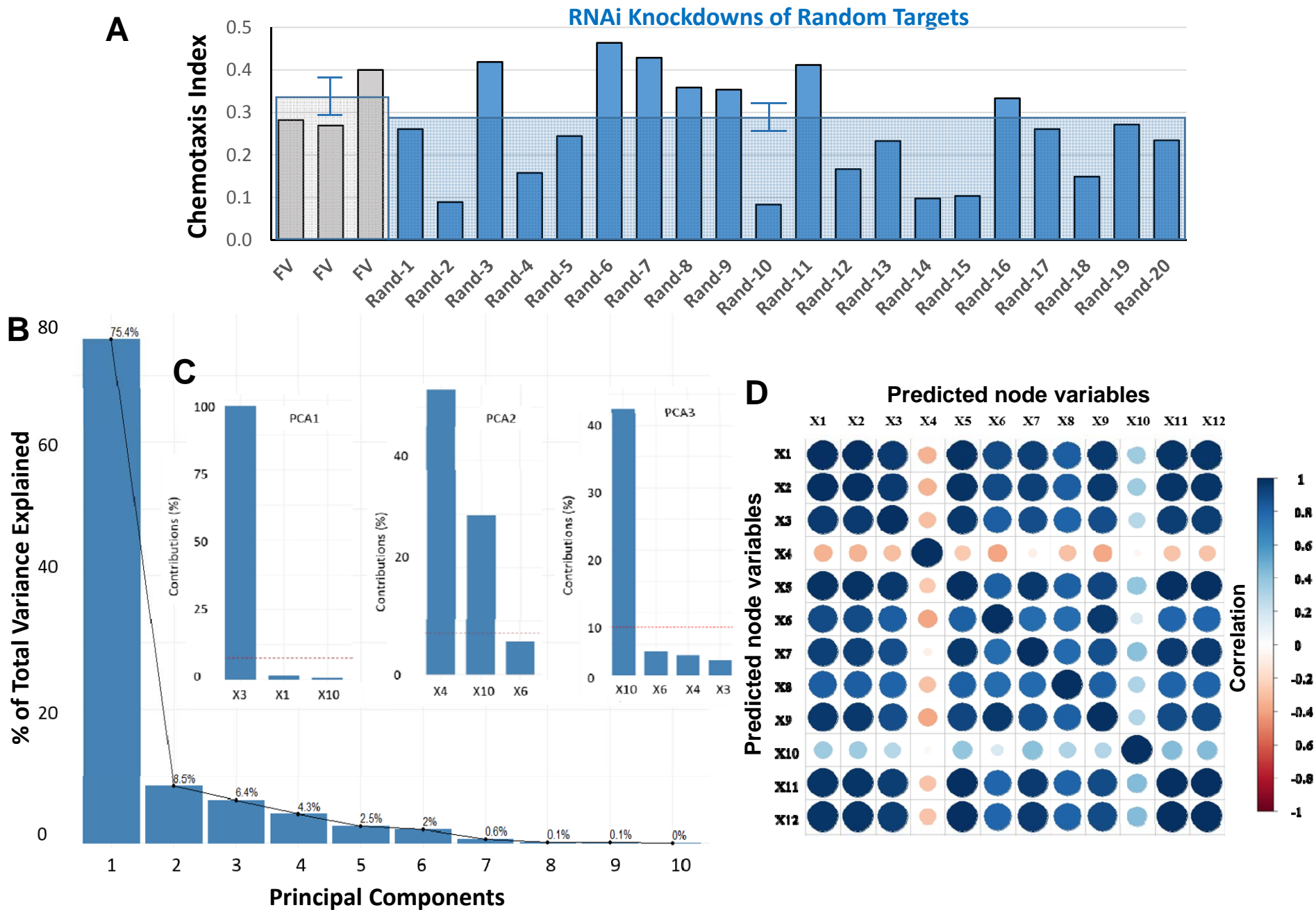
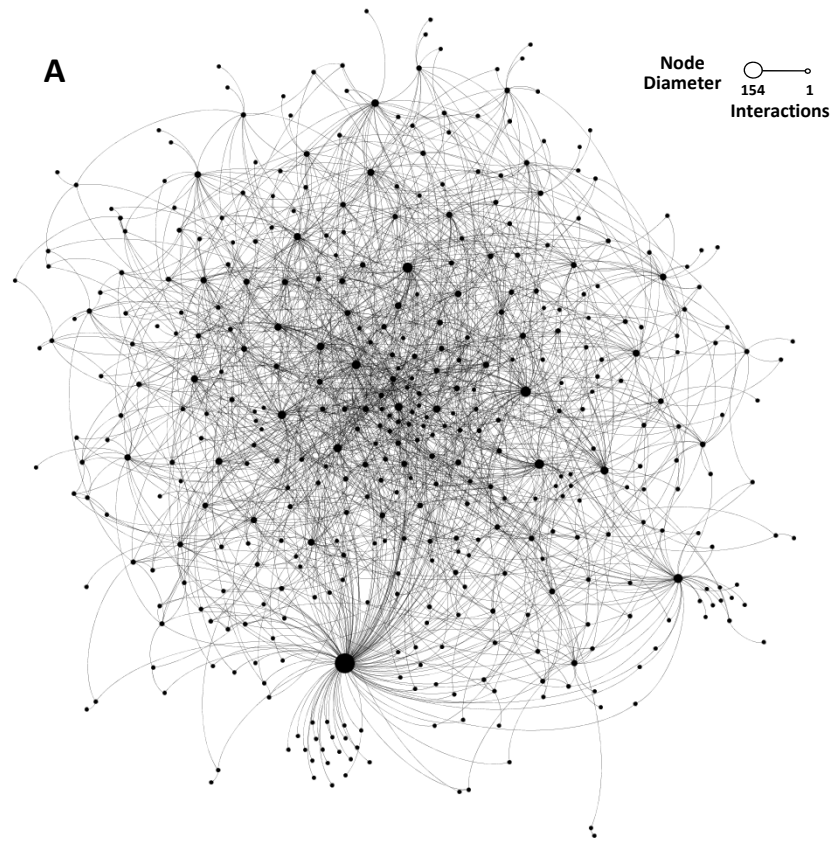
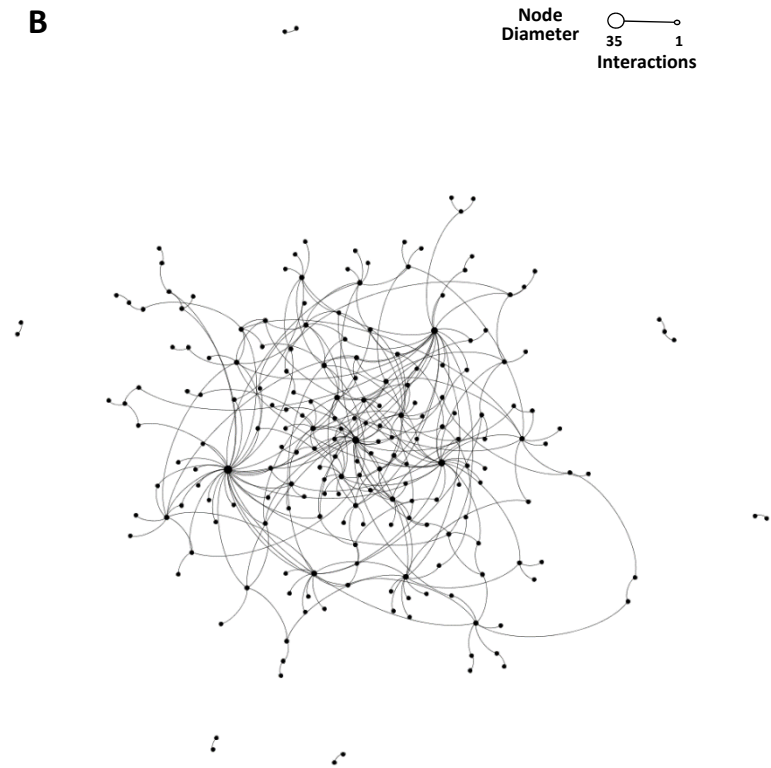


Figure S2



Without ASA treatment: Interactions common between SY5Y and SY5Y-APP<sub>Sw</sub>



After ASA treatment: Interactions common between SY5Y and SY5Y-APP<sub>Sw</sub>

**Figure S1: Principal components analysis of parameters that predict chemotaxis rescue in a *C. elegans* model of amyloidosis due to leaky neural expression of human A $\beta$ <sub>1-42</sub> (related to Figure 4)**

(A) Normalized chemotaxis indices of 5-day-old *C. elegans* adults fed 20 random RNAi constructs. Strain CL2355, with leaky [uninduced] pan-neuronal expression of human A $\beta$ <sub>42</sub>, derived no significant protection against chemotaxis decline, relative to empty-feeding-vector (FV) controls, in marked contrast to the protection conferred when targeting proteins implicated by the aggregate contactome (Figure 4A; of 22 proteins knocked down, 8 gave significant rescue by *t* test, 12 by Chi<sup>2</sup>).

(B) Principal Components Analysis (PCA) of the 12 predicted node-protein parameters. Bar height for each orthogonal component shows its contribution to Chemotaxis Index (C.I.) as % of variance explained. Components 1 – 3 account for >90% of total C.I. variance.

(C) Contributions of node variables (X1 – X12) to each of the first 3 principal components. X1=degree (number of interactions); X3 = number of triangles; X4 = Clustering Coefficient; X10 = protein molecular weight.

(D) Cross-correlations among input parameters X1 – X12. Size and shading of circles indicate the strength of positive (blue) or inverse (red) correlation, as indicated by the scale at panel right. Note that degree (X1), Clustering Coefficient (X4), and molecular weight (X10) showed negligible cross-correlation to one another.

**Figure S2: Aggregate contactomes for SY5Y-APP<sub>sw</sub> cell aggregates, restricted to protein-protein crosslinks shared in common with SY5Y aggregates (related to Figures 1C and 6C).**

Aggregates were isolated and analyzed exactly as for Figure 1C (corresponding to Figure S2A) and Figure 6C (corresponding to Figure S2B), with the sole additional criterion that interactions were included only if they met the thresholds for both SY5Y-APP<sub>sw</sub> and SY5Y aggregates (e.g., black edges in Figure 1C).

(A) Aggregate interactions for untreated SY5Y-APP<sub>sw</sub> cells.

(B) Aggregate interactions for SY5Y-APP<sub>sw</sub> cells exposed to 0.5-mM aspirin for 48 hours.

**Table S1. Parameters that best predict RNAi rescue of declining Chemotaxis Index (C.I.), in a *C. elegans* model of AD-like amyloidopathy (related to Figures 4 and S1)**

Protein	Degree	Clustering Coefficient (CC)	Mol.Wt.	Degree x CC	MW x CC	Experimental C.I.	Predicted C.I. (Neural Network)
EIF3A	144	0.14	152.0	19.71	20.80	2.20	2.19
SRSF6	156	0.09	37.8	14.63	3.55	1.72	1.73
RFC1	85	0.21	126.3	17.50	26.00	2.41	2.33
TRIPC	76	0.21	219.1	16.13	46.51	1.56	1.74
SNUT1	91	0.14	88.0	13.00	12.57	1.97	1.76
ZN292	76	0.19	299.5	14.72	58.01	1.87	1.74
ASPM	94	0.10	382.5	9.14	37.19	1.79	1.71
CHD1	66	0.17	98.7	11.45	17.11	1.68	1.63
NUCL	37	0.22	78.1	8.28	17.47	1.53	1.50
DDX52	21	0.30	65.9	6.30	19.77	1.72	1.83
ROA3	12	0.14	41.6	1.64	5.67	2.03	1.88
SF3A3	10	0.22	55.1	2.22	12.25	1.78	1.88
ACTN1	12	0.14	98.1	1.64	13.38	1.98	1.75
RS5	8	0.00	38.7	0.00	0.00	1.72	1.98
DRG1	4	0.00	43.3	0.00	0.00	1.91	2.04
COPG1	4	0.00	96.1	0.00	0.00	2.12	2.03
ANK2	49	0.18	93.6	8.75	16.72	2.21	1.42
CLH1	11	0.44	184.3	4.80	80.40	1.97	2.10
E41L3	13	0.28	119.6	3.67	33.72	1.64	1.88
LAMB	9	0.25	197.8	2.25	49.45	2.64	2.30
LMNA	14	0.36	73.0	5.08	26.49	2.17	2.28
UBA1	11	0.25	41.9	2.80	10.67	1.63	1.90
TAU	13	0.38	83.4	5.00	32.07	2.70	2.45
SERF2	6	0.27	6.9	1.60	1.84	1.92	2.10
PRP8	74	0.14	256.9	10.14	35.18	1.13	1.39
RNPS1	87	0.16	33.6	14.09	5.43	1.67	1.97
PRP4B	140	0.08	110.8	10.66	8.44	1.29	1.31
IF2B	8	0.21	63.5	1.71	13.60	2.33	1.93
TOP2B	57	0.19	178.9	10.86	34.07	1.70	1.40
RBBP6	121	0.13	197.1	16.17	26.34	1.58	1.65
KMT2A	96	0.14	436.6	13.92	63.29	1.73	1.80
NFM	33	0.23	100.8	7.75	23.66	1.31	1.46
EIF3B	7	0.24	89.5	1.67	21.32	1.82	1.97
APP	8	0.32	9.8	2.57	3.15	2.43	2.26
CKAP5	46	0.27	223.5	12.27	59.61	1.70	1.71

**C.I. = Fold-change in chemotaxis index upon RNAi knockdown, relative to F.V. controls**

The Pearson correlation coefficient between C.I. values observed experimentally, and those predicted by a neural-network algorithm from the above node parameters, was 0.77 ( $P < 0.0001$ ).

## Transparent Methods

### Cell culture and maintenance

Human neuroblastoma cell lines SH-SY5Y and SH-SY5Y-APP<sub>Sw</sub> (SH-SY5Y cells expressing the “Swedish” familial-AD mutant form of amyloid precursor protein (APP) (Balasubramaniam et al., 2018)), were maintained in culture dishes containing DMEM-F12 (1:1) nutrient mixture (Ham’s F-12 Medium) supplemented with 10% v/v fetal bovine serum. Cultures were held at 37±0.2°C with 5% CO<sub>2</sub> in a tissue-culture incubator. Except before and during cross-linking or aspirin treatments, culture media also contained 1% v/v of a penicillin-streptomycin stock (5000 units/ml and 5 mg/ml, respectively; ThermoFisher). For aggregate preparation and cross-linking studies, well-maintained cells were grown to 70% confluence, then detached in trypsin/EDTA, flash frozen under liquid nitrogen in DPBS, and stored at –80°C. Aspirin (ASA) was added to SY5Y-APP<sub>Sw</sub> cells as indicated, at 0.5-mM for 48 h just prior to trypsin digestion and freezing, as detailed above.

### Nematode strains and maintenance

*C. elegans* strain CL2355 [*smg-1<sup>ts</sup>* (*snb-1/Aβ<sub>1-42</sub>/long 3’-UTR*)], expressing human Aβ<sub>1-42</sub> in all neurons, serves as a model of Alzheimer-like amyloidosis. CL2355 was obtained from the Caenorhabditis Genetics Center (CGC), stored as frozen larval cultures at –70°C, and once thawed, maintained at 20°C on solid nematode growth medium (NGM) overlaid with *E. coli* (strain OP50). For gene knockdown, worms (well-fed for ≥2 generations) were lysed on day 3 post-hatch and eggs were placed on plates with lawns of *E. coli* expressing RNA-interference constructs from the Ahringer library (Kamath and Ahringer, 2003).

### Synthesis of crosslinker-1 (Cross-linking reagent):

Nitromethyltrispropionic acid (**1**, 0.50 g, 1 eq. 1.80 mmol), *N*-(3-dimethylaminopropyl)-*N'*-ethylcarbodiimide hydrochloride (EDC, 1.10 g, 3.2 meq., 5.7 mmol) and *N*, *N*-diisopropyl-ethylamine (1 mL, 3.2 eq., 5.7 mmol) were added to dry dioxane (10 mL) at 20-25°C under an argon atmosphere. The stirred reaction mixture was heated at 20-25°C for 10 min followed by the addition of *N*-hydroxysuccinimide (**2**, 0.64 g, 3.1 eq., 5.56 mmol). The reaction mixture was stirred for 24 hr or until completion of the reaction (monitored by thin-layer silica-gel chromatography; 100% ethyl acetate mobile phase, product visualization with potassium permanganate spray; R<sub>f</sub> = 0.9). After completion of reaction, the mixture was concentrated under gradually reduced pressure

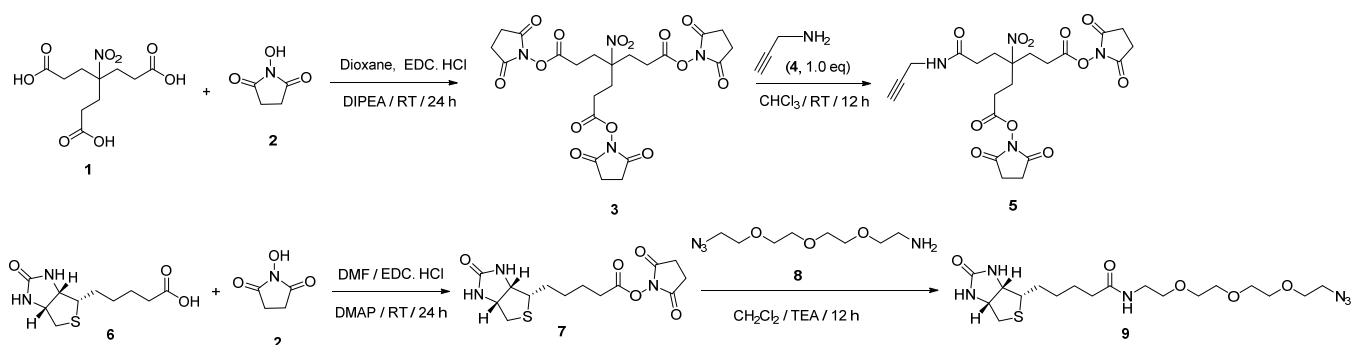
(400 to 30 mm Hg) at 40°C to remove dioxane. The residue was dissolved in ethyl acetate (50 mL), washed with water (2x20 mL), and the separated ethyl acetate layer dried over anhydrous sodium sulfate, filtered and concentrated under reduced pressure to remove the ethyl acetate. The resulting product was precipitated from diethyl ether, filtered, and dried under vacuum to afford compound **3** (Yield: 91%, 0.93 g).

The above tri-NHS ester of nitromethyltrispropionic acid (**3**, 0.90 g, 1 eq., 1.58 mmol) was suspended in a stirred, dry chloroform solution containing propargylamine (**4**, 0.1 mL, 1 eq., 1.58 mmol) under a nitrogen atmosphere at 20-25 °C for 12 hrs. The reaction mass was concentrated by removal of chloroform under gradually reduced pressure (400 → 100 mm Hg) and the resulting residue was extracted into ethyl acetate and washed with ice-cold water (2x10 mL). The separated ethyl acetate layer was washed twice with 1-M phosphate buffer, pH 7.0, and dried over anhydrous sodium sulfate, filtered, and concentrated under reduced pressure to remove the ethyl acetate. The resulting residue was not purified through a silica gel column, because it was previously reported that crosslinker-1 (**5**) undergoes hydrolysis during silica gel chromatography. The residue was dried under vacuum to obtain the crude crosslinker-1 (**5**, Yield: 65%, 0.52 g, ~90% pure from NMR analysis). The NMR spectral data (<sup>1</sup>H and <sup>13</sup>C spectra) were consistent with the reported NMR values (Chowdhury et al., 2009).

#### **Synthesis of crosslinker-2 (cross-linking enrichment reagent):**

Biotin (**6**, 1g, 1 eq., 4.09 mmol) was dissolved in dimethyl formamide (DMF; 5 mL), and *N*-(3-dimethylaminopropyl)-*N'*-ethylcarbodiimide hydrochloride (EDC, 0.94 g, 1.2 eq., 4.91 mmol) and *N,N*-diisopropylethylamine (0.79 mL, 1.3 eq., 5.32 mmol) added under an argon atmosphere at 20–25°C. The mixture was stirred 10 min prior to addition of *N*-hydroxysuccinimide (**2**, 0.47 g, 1.0 eq., 4.09 mmol). The reaction mixture was then stirred for 24 hrs at 20–25°C and progress of the reaction was monitored by thin-layer silica gel chromatography. After reaction completion, the products were concentrated under reduced pressure to remove DMF. Isopropyl alcohol (50 mL) was then added and the mixture stirred for 10 minutes to form a white precipitate, which was filtered and dried under vacuum to afford compound **7** (Yield: 93%, 1.29 g). The NMR spectral data (<sup>1</sup>H and <sup>13</sup>C-spectra) for compound **7** were consistent with the reported NMR values (Kang et al., 2009).

NHS-biotin (0.30 g, 1 eq., 0.87 mmol) was added to a dichloromethane (5 mL) solution of 11-azido-3,6,9-undecanamine (**8**, 0.19 g, 1 eq., 0.87 mmol) under nitrogen, and a catalytic amount of triethylamine was added. The resulting reaction mixture was stirred for 12 hr at room temperature under nitrogen and monitored by thin-layer silica-gel chromatography (with 8% MeOH in dichloromethane as solvent). After completion of the reaction, the mixture was washed with water (2x5 mL), and the separated organic layers combined and dried over anhydrous sodium sulfate, filtered and evaporated to dryness to afford crosslinker-2 (**9**, yield: 80%, 0.31 g). Compound **9** was characterized by  $^1\text{H}$ ,  $^{13}\text{C}$ -NMR and mass spectra. The NMR spectral data of compound **9** were consistent with the reported NMR values (Li and Zuilhof, 2012; Wang et al., 2009).



### Purification of insoluble aggregates

Frozen cells (SY5Y, SY5Y-APP<sub>Sw</sub>, and SY5Y-APP<sub>Sw</sub> treated with ASA) were pulverized in a Kontes homogenizer, cooled on dry ice. Cell lysis buffer containing inhibitors of proteases and phosphatases was added to crushed, frozen cells as described (Ayyadevara et al., 2017). Cell debris was removed by a brief low-speed centrifugation (5 min, ~1800 g), and total protein was assayed with Bradford reagent (Bio-Rad). Equal protein contents were taken and total aggregates were separated from cytosol by a medium-speed centrifugation (18 min, 18000 rpm). Supernatant (cytosolic fraction) was carefully discarded, and 1% v/v sarcosyl buffer was added to the pellet (total aggregate fractions), as described (Ayyadevara et al., 2017), and incubated for 20 mins at 4°C with gentle shaking. Detergent-insoluble fractions were recovered by high-speed centrifugation (30 min, 90,000 g) and further processed for cross-linking.



### **Chemical cross-linking of insoluble aggregates**

The procedure of Chowdary et al. (Chowdhury et al., 2009) was modified for click-labelling of aggregate proteins and peptide-pair enrichment. Cross-linking reagent propargyl amine was prepared in DMSO, a final concentration of 5 $\mu$ M was added to the insoluble fractions in 20-mM PBS (pH 7.5), and incubated for 30 min at room temperature. The reaction was quenched with 50-mM Tris-HCl (pH 8.0) and cross-linked samples were centrifuged 30 min at 90,000  $\times$  g, 4°C, to remove excess unbound cross-linker (in the supernatant).

### **Tryptic digestion of cross-linked aggregates**

Cross-linked aggregates were incubated in buffer containing 8M urea and 122mM DTT, for 30 min at 37°C., followed by a 20 min incubation in dark at 22°C in the presence of 40mM iodoacetamide. To the reduced sample of protein aggregates 10 units of trypsin (Pierce) was added along with 150mM ammonium bicarbonate and incubated overnight at 37°C. Reaction was then quenched by addition of 3% glacial acetic acid.

### **Isolation of crosslinked peptides**

The tryptic peptides are desalted using 1cc C18 column (Sep-Pak, Waters) containing 50mg of resin. Recovered peptide fractions were evaporated to dryness (Speed-Vac, ThermoFisher) and reconstituted in biotin crosslinker containing 0.25-mM TBTA (Tris [(1-benzyl-1H-1,2,3-triazol-4-yl) methyl]amine, 250 $\mu$ M CuSO<sub>4</sub>, 5-mM Tris-phosphine buffer, and 1:10 molar ratio of biotin crosslinker azide solution and incubated at 40°C for 2 hours to facilitate alkyne azide cycloaddition. Biotin attached crosslinked peptides were isolated with streptavidin coated magnetic beads according to manufacturer's instructions (ThermoFisher). Streptavidin bound peptides were eluted in buffer containing 50% acetonitrile and 0.4% Trifluoroacetic acid after brief washes with PBS.

### **LC-MS/MS analysis of cross-linked peptides**

Tryptic peptides were separated on a reverse-phase C18 column (120  $\times$  0.075 mm, particle size 2.5 $\mu$ m; Waters XSelect CSH) utilizing an Ultimate 3000 RSLCnano liquid chromatography system (Thermo). Peptides were eluted over a 30 min gradient from 97:3 to 67:33 buffer (A:B ratios, where buffer A contains 0.5% acetonitrile, 0.1% formic acid in LCMS-grade water, and buffer B contains 0.1% formic acid in LCMS-grade acetonitrile). Eluted peptides were ionized by

electrospray (2.15 kV) prior to mass spectrometric analysis on an Orbitrap Fusion Tribrid mass spectrometer (Thermo). MS data were acquired using the FTMS analyzer in top-speed profile mode at a resolution of 4 parts per million over a range of 375 – 1500 m/z. Following CID activation with normalized collision energy of 35.0, MS/MS data were acquired for each peptide using the ion-trap analyzer in centroid mode with three sequential activation settings: HCD activation with normalized collision energy of 28.0, ETD activation with calibrated charge-dependent parameters, and EThcD supplemental activation.

### **Mass-spectrometry data analysis**

Cross-linked peptides from LC-MS/MS spectra were analyzed using Xlink-Identifier (Du et al., 2011). Because the original Xlink-Identifier software does not support parallel processing of data, we developed a Linux-based, in-house script to partition the data and route them to 32 CPUs in parallel for Xlink-Identifier screening. Prior to running Xlink-Identifier, the list of proteins to be considered as potential contributors of crosslinked peptides (the reference database) was compiled from a proteomic analysis of sarcosyl-insoluble aggregates from SY5Y and SY5Y-APP<sub>Sw</sub> cells, as described previously (Ayyadevara et al., 2017). Only proteins with  $\geq 3$  spectral hits were included in the reference database used for Xlink-Identifier analysis. To eliminate minor and irreproducible linkages, we incorporated two stringent criteria: (i.) an interlinked peptide should have  $\geq 10$  spectral hits, and (ii.) the observed protein-protein pair must be present in at least 2 of 3 cross-linking experiments. All data analyses were performed using in-house Linux shell scripts.

### **Modeling of protein-interaction networks**

Results from Xlink-Identifier data analysis were processed by GePhi<sup>TM</sup> (Bastian et al., 2009) and Orange<sup>TM</sup> (Demsar et al., 2013) software packages to model and visualize, respectively, the aggregate interactome. To define characteristic parameters (predictors) for each node, including degree (number of interacting partners) and eigenvector centrality, we used a graph-modeling statistical plugin from GePhi and a network module in the Orange package.

### **Multivariate-linear-regression and neural-network analyses**

Principal component analysis (PCA) and stepwise, forward/reverse multivariate linear regression were performed within their respective R modules. PCA identifies orthogonal input-parameter clusters to collapse highly correlated predictors into a minimal number of uncorrelated predictor

dimensions computed from network graphs for the nodes of interest. Conventionally, PCA (the `prcomp` function in R) centers the molecular descriptors to have means of zero; we also normalized the variables to have standard deviations of 1. PCA applies linear transformations to fit the 13 predictors into a coordinate system in which the most significant variance is found on the first coordinate (PC1), and each successive coordinate is orthogonal to all others and accounts for a smaller fraction (%) of total variance (R Core Team, 2013). The first three PCs accounted for 75.4%, 8.5%, and 6.4%, respectively, of the total variation in the dataset, thus together explaining >90% of total variance. Even in 2 dimensions, the data provide a close approximation to the original resolution of groups in 13-dimensional space.

The input variables that contributed substantially to PC1 – PC3 were used to build a stepwise, forward-backward multi-variate linear regression (F/R-MLR) model. Model fitting utilized the Akaike information criterion to evaluate the impacts of stepwise additions and removals of independent variables in the model using “`stepAIC`” and “`lm`” functions in R (Zeileis et al., 2002). MLR models included 3 individual parameters and all possible combinations of interaction terms (totaling 8 variables) as predictor variables. Data were randomly partitioned (70/30) into training and testing sets. A leave-one-out protocol was also employed for cross-validation of the top-ranked model, to determine the adjusted percent of variance explained by the correlation between predicted and actual chemotactic index (C.I.). After stepwise addition and subtraction, the final model consisted of 3 independent variables and 2 interactions (between degree and MW, and CC and MW), with fold-change in chemotaxis as the dependent variable or prediction target.

We selected the MLR model with the lowest root-mean-square deviation from a linear regression (0.3), requiring  $P < 0.001$ , to define inputs for neural-network prediction — which is inherently both nonlinear and nonparametric.

For neural network training and predictions, we employed a multilayer perceptron (MLP) algorithm with back-propagation, implemented as an Orange<sup>TM</sup> module (Demsar et al., 2013). The same dataset used for MLR prediction of the chemotaxis index was again randomly split 70:30 into training and testing sets, over 50 iterations. Our neural network algorithm utilized 100 neurons per hidden layer, the activation method was set to ReLu, and solver was selected as Adam (Demsar et al., 2013). RMSE for the neural-network training was 0.4. At the conclusion of the learning and testing iterations, the chemotaxis index (normalized as fold change) was predicted and plotted for the full dataset.

## Chemotaxis assay

Chemotaxis was assessed in strain CL2355 (pan-neuronal expression of A $\beta$ <sub>1-42</sub>) as previously described (Ayyadevara et al., 2015). Briefly, eggs from age-synchronized cohorts of worms were fed from hatch with either empty feeding vector (FV) with or without ASA, or with bacteria carrying a plasmid that transcribes complementary exonic RNA strands to direct RNA interference against the gene of interest (Ayyadevara et al., 2015; Kamath and Ahringer, 2003). Worms were maintained at 20°C without acute induction but exhibiting age-dependent loss of chemotaxis (Ayyadevara et al., 2015). ASA stock solution was 100 mM in 95% (v/v) ethanol; prior to each treatment it was diluted to 1 mM in nematode growth medium (NGM). Worms from day 5 (post-hatch) were collected after serial washes to remove any bacteria, and were assayed as previously described (Ayyadevara et al., 2017) in 100 mm culture dishes. Chemotaxis toward 1-butanol was scored after 2 hours and the ‘Chemotaxis Index’ (CI) was calculated as a normalized response.

## Thioflavin-T staining of SY5Y-APP<sub>sw</sub> cells

To assess amyloid-like aggregates, SY5Y (wild-type) and SY5Y-APP<sub>sw</sub> were stained using thioflavin-T as described previously (Balasubramaniam et al., 2018). Briefly, cells at 70–80% confluence were detached in trypsin/EDTA and sub-cultured in 4-chamber slides (10,000–15,000 cells/chamber) containing antibiotic-free DMEM medium with 10% FBS (Invitrogen). SY5Y-APP<sub>sw</sub> cells were treated with 0.5-mM ASA or vehicle alone, and maintained at 37°C for 48 hours. Cells were then fixed (4% v/v formaldehyde), and then incubated with 0.1% (w/v) thioflavin T in phosphate-buffered saline (PBS) along with DAPI. Fluorescence intensities of images captured on a Nikon Eclipse *Ti* microscope were quantified using in-house FIJI (imageJ) scripts.

## Protein-protein and protein-ligand docking

The structures of proteins featured in **Figure 2, C&D**, were obtained from PDB (Protein DataBase). Proteins represented in **Figure 6, F-J**, were modelled in 3 dimensions using Modeller (by homology modeling) or fold recognition and *ab-initio* methods (implemented by the iTASSER server) (Yang and Zhang, 2015), with the exception of controls in **Figure 6F**, for which structures were obtained from PDB. Protein-protein docking was modeled by the Hex 6.1 program, based on shape and electrostatic charge complementarity as previously described (Balasubramaniam et al., 2018; Ritchie et al., 2008), with other docking parameters set to default. To analyze ASA

interactions, protein-ligand docking was implemented in AutoDock-Vina (Linux based) using the Raccoon (Windows) interface. The lowest docking-energy ( $\Delta G_{\text{binding}}$ ) pose was taken as the best model. Results were analyzed and plotted using the Discovery Studio visualizer (BIOVIA, Dassault Systemes, San Diego [2017])

### Statistical analyses

We compared groups of replicate samples by 2-tailed  $t$  tests if group size was  $>10$  (e.g., **Figures 1B and 6B**), or Behrens-Fisher (heteroscedastic)  $t$  tests for smaller samples in which variance was unknown or may be unequal. In some instances, when the direction of change is known or strongly predicted, a 1-tailed  $t$  test may be substituted. Differences in proportions were assessed within an experiment by Chi-squared ( $\text{Chi}^2$ ) or Fisher Exact tests (e.g., asterisks in **Figure 4A**). If replication is sufficient, ratios from individual experiments may be treated as points within groups, which can then be compared by heteroscedastic  $t$  tests (e.g., numbers above bars in **Figure 4A**).

In experiments with multiple end-points, Bonferroni corrections have not been applied, leaving it to the reader to compare the frequency of “positives” to their expected frequency (e.g., 5% at  $\alpha = 0.05$ ).

### Network parameters

Two of the standard descriptors used widely to characterize local network properties are the Clustering Coefficient (CC), by which we here mean the local, undirected clustering coefficient, as the fraction of triplets (potential node-triangles) directly connected to that node, that form closed triangles of 3 interconnected nodes [51]. For any vertex  $v_i$  (node  $i$  with at least 2 interacting partners),  $CC_i$  is calculated as  $CC_i = \frac{2|\{e_{jk} : v_j, v_k \in N_i, e_{jk} \in E\}|}{k_i(k_i - 1)}$  where  $v_j$  and  $v_k$  are vertices directly connected to  $v_i$  (Watts and Strogatz, 1998). Eigenvector centrality (EC) reflects node connectivity to high-degree hubs, comprising both direct and indirect connectivity. EC is calculated as  $x_v = \frac{1}{\lambda} \sum_{t \in M(v)} x_t = \frac{1}{\lambda} \sum_{t \in G} a_{v,t} x_t$  where  $M(v)$  is the set of the neighbors of vertex  $v$ , and  $\lambda$  is a constant (<https://gephi.org>). Highly influential hub connectors are those for which  $CC/EC \leq 100$ , using normalized EC values (Watts and Strogatz, 1998).